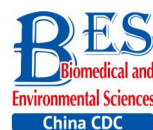


## Original Article



# Biocompatibility and Immunotoxicology of the Preclinical Implantation of a Collagen-based Artificial Dermal Regeneration Matrix\*

WANG Wei<sup>1</sup>, ZHANG Lin<sup>2</sup>, SUN Lei<sup>2</sup>, SHE Zhen Ding<sup>3</sup>, TAN Rong Wei<sup>3</sup>, and NIU Xu Feng<sup>4,#</sup>

1. Department of Immunology, School of Basic Medical Sciences, NHC Key Laboratory of Medical Immunology, Peking University, Beijing 100191, China; 2. Beijing Advanced Innovation Center for Biomedical Engineering, Key Laboratory for Biomechanics and Mechanobiology of Ministry of Education, School of Biological Science and Medical Engineering, Beihang University, Beijing 100083, China; 3. Shenzhen Lando Biomaterials Company Limtd, Shenzhen 518107, China; 4. Research Institute of Beihang University in Shenzhen, Shenzhen 518057, China

## Abstract

**Objective** Graft rejection, with the possibility of a violent immune response, may be severe and life threatening. Our aim was to thoroughly investigate the biocompatibility and immunotoxicology of collagen-based dermal matrix (DM) before assessment in clinical trials.

**Methods** DM was subcutaneously implanted in BALB/c mice in two doses to induce a potential immune response. The spleen and lymph nodes were assessed for shape, cell number, cell phenotype via flow cytometry, cell activation via CCK8 kit, Annexin V kit, and Ki67 immunostaining. Serum samples were used to measure antibody concentration by enzyme-linked immunosorbent assay. Local inflammation was analyzed by histology and immunohistochemistry staining. Data analysis was performed by one-way ANOVA and non-parametric tests.

**Results** Our data illustrate that the spleen and lymph node sizes were similar between the negative control mice and mice implanted with DM. However, in the high-dose DM (DM-H) group, the total cell populations in the spleen and lymph nodes, T cells and B cells in the spleen had slight increases in prophase, and the low-dose DM (DM-L) group did not display gross abnormalities. Moreover, DM-H initiated moderate cell activation and proliferation in the early phase post-immunization, whereas DM-L did not. Neither DM-H nor DM-L implantation noticeably increased IgM and IgG serum concentrations. Examination of the local cellular response revealed only benign cell infiltration and TNF- $\alpha$  expression in slides of DM in the early phase.

**Conclusion** Overall, DM-H may have induced a benign temporary acute immune response post-implantation, whereas DM-L had quite low immunogenicity. Thus, this DM can be regarded as a safe product.

**Key words:** Collagen; Lymphocytes; Immunogenicity; Flow cytometry

Biomed Environ Sci, 2018; 31(11): 829-842

doi: 10.3967/bes2018.110

ISSN: 0895-3988

www.besjournal.com (full text)

CN: 11-2816/Q

Copyright ©2018 by China CDC

\*This study was supported by the National Natural Science Foundation of China [No. 31470915]; Shenzhen Science and Technology Project [No. JCYJ20170817140537062]; the Fundamental Research Funds for the Central Universities [No. YWF-18-BJ-J-217]; and the 111 Project [No. B13003].

#Correspondence should be addressed to NIU Xu Feng, E-mail: nxf@buaa.edu.cn

Biographical note of the first author: WANG Wei, female, born in 1983, PhD in immunology, associate professor, majoring immunology.

## INTRODUCTION

Immune rejection is a reaction of the immune system that aims to resist foreign substances. Graft rejection consists of host versus graft reaction and graft versus host reaction, and the former is classified into hyperacute rejection, acute rejection, and chronic rejection<sup>[1]</sup>. Clinical hyperacute rejection generally leads to graft non-function, but in cardiac transplantation, its occurrence may cause death<sup>[2-3]</sup>; acute rejection is the most common reaction, manifesting as a sudden graft function deterioration, whereas chronic rejection is characterized by graft fibrosis and dysfunction<sup>[4-5]</sup>. Tissue matching before transplantation<sup>[6]</sup>, immunosuppressive therapy<sup>[7-8]</sup>, and immunological monitoring<sup>[9]</sup> are important and effective methods to avoid and lessen the chance of graft rejection in the clinic. For implantable biomedical devices, biocompatibility and immunotoxicology evaluations in animals are regarded as another effective strategy to reduce adverse effects in the clinic.

Collagen is considered one of the most useful biomaterials and extensively applied in drug release systems and tissue repair<sup>[10]</sup>. It is widely applied in skin repair and reconstruction because collagen is the major constituent of the dermal matrix (DM) and has excellent biocompatibility, low immunogenicity and cytotoxicity, cell adhesion, biodegradability, and availability<sup>[11-12]</sup>. Nevertheless, for animal-sourced collagen, there exists a growing concern regarding transmissible diseases<sup>[13]</sup>. In addition, the purity of collagen, extraction methods, crosslinking methods, and implantation sites may complicate the immunogenicity of collagen<sup>[14]</sup>. It should be noted that an excessive immune response may destroy the body's immune function and trigger immune toxicity, which could be life threatening. Therefore, immunological evaluations of any medical products based on collagen are essential and urgently needed.

In previous studies<sup>[15-19]</sup>, *ex vivo* and *in vivo* experiments were performed for the biological evaluation of biomaterials. *In vitro* tests mainly include assessments of cell attachment, cell proliferation, and cell apoptosis. For *in vivo* tests, enzyme-linked immunosorbent assay (ELISA) to determine antibody and cytokine levels and histological and immunohistochemistry staining are the primary measurements. Nonetheless, most researches only used at most two methods, and a comprehensive and systemic research scheme is

lacking for the immunological evaluation of biomedical materials. Therefore, a scheme involving systematic and local responses, cellular and humoral immune responses, and innate and adaptive immunities was designed to investigate the biocompatibility and immunotoxicology of artificial dermal regeneration matrix in this study. This study was conducted based on ISO 10993 and the previous literature<sup>[20]</sup>. This investigation will aid in controlling adverse responses elicited by DM in the clinic and provide reference for immunogenicity evaluations of other biomedical materials.

## MATERIALS AND METHODS

### Materials and Animals

The DM and positive control (PC), bovine tendon, used in this study were supplied by Shenzhen Lando Biomaterials Co. Ltd. This product is used to repair skin damaged by third-degree burns, cerebral surgeries, and dermal defects. This DM consists of two layers: the top layer is silicone and tears off after a period of time, whereas the bottom layer is an artificial collagen-based dermal regeneration matrix. The bottom layer is the research subject of this study. It is porous and fabricated with collagen (over 95%)-chondroitin sulfate using a bionic design. Because chondroitin sulfate is favorable for cell adhesion, wound healing, and skin regeneration and because chondroitin sulfate is nonimmunogenic<sup>[21-22]</sup>, the addition of chondroitin sulfate gives the DM a better degradation performance and thermodynamic property to enhance cell adhesion and proliferation. For collagen immunotoxicity control, three measures were taken: First, because telopeptides are among the antigenic determinants of collagen, the collagen used in this product was telopeptide-removed collagen; second, crosslinking by aldehydes to block antigens similar to  $\alpha$ -Gal glycoprotein, which can trigger an acute immune rejection reaction; and third, high-temperature crosslinking was performed to remove resident DNA.

All procedures performed in studies involving animals were in accordance with the Institutional Animal Ethics Committee of Peking University Health Science Center. A total of 100 BALB/c female mice (Beijing Vital River Laboratory Animal Technology Co., Ltd), aged 6 to 8 weeks old and with a weight of 17-22 g, were used in this experiment. Five mice were allocated randomly to each group and each time point as duplicate samples. In this study, the

experimental groups comprised the high-dose DM (DM-H) group and low-dose DM (DM-L) group. In addition, a group with no implant and another group with bovine tendon implants were set as the negative control (NC) group and PC group.

DM-L was calculated based on the maximum dose typically applied in the clinic per time and the body surface area ratio of BALB/c mice to humans, and DM-H was 4-fold higher than DM-L. According to the Stevenson formula, body surface area ( $m^2$ ) =  $0.0061 \times \text{height} + 0.0128 \times \text{weight} - 0.1529$ . According to the Meeh-Rubner formula, animal body surface area =  $K \frac{W^{2/3}}{1000}$ , where K is a constant, K is 9.1 for mice and rats, and W is the weight, in g. As a result, the area of DM-H and DM-L was  $1.25 \text{ cm} \times 2.5 \text{ cm}$  and  $1.25 \text{ cm} \times 0.625 \text{ cm}$ , respectively. As DM is made of purified bovine tendon type I collagen, the PC group was implanted with unpurified bovine tendon to elicit an obvious immune response. The dose of bovine tendon was based on DM-H; thus, means DM-H and the dose of bovine tendon contained the same quantity of collagen to assure an intense immune response in the PC group.

### Surgeries

Prior to each surgery, 0.5% (w/v) sodium pentobarbital (Sigma) in saline solution was injected intraperitoneally at 50 mg/kg to anesthetize mice. Mice were placed into a prone position to perform one implantation on one side of the spine. After being shaved, the skin was disinfected with 75% alcohol. A 1 cm cut was made through the skin, an implant (no implant for the NC group) was inserted into this incision, and the wound was closed with an absorbable PGA suture<sup>[23-24]</sup>. Each mouse was subcutaneously implanted three times in total, once each week. After three immunizations (same meaning as 'implantations' in this study), the mice were kept for 7, 14, 30, 60, and 90 days before being sacrificed. At 3 days post-implantation, blood was collected in EP tubes after cutting the tails. On each harvesting day (days 7, 14, 30, 60, 90), blood was collected by extracting one eyeball before the mice were sacrificed. Serum and blood cells were separated by centrifugation at 10,000 rpm for 5 min, and then, serum was stored at -20 °C for antibody analysis. Following cervical dislocation, the skin at the defect sites was sheared and fixed in 4% paraformaldehyde for histological analysis. Under sterile conditions, the spleen and lymph nodes close to the wounds were extracted and immersed in

sterile phosphate buffer solution (PBS) for further processing.

### Immune Organ Processing and Cell Counting

The spleens and lymph nodes in the NC group, PC group, and each DM group were photographed. Cell suspensions were prepared by grinding the spleens and lymph nodes and filtering through 40  $\mu\text{m}$  cell strainers in an aseptic environment. Erythrocytes in spleen cells were lysed by adding red blood cell lysis buffer for 1 min before counting<sup>[25]</sup>. Following red blood cell lysis, splenic immune cells were collected by centrifuging at 800 rpm for 10 min. After resuspending in PBS, splenic immune cells were counted with an automatic blood cell counter. Lymph node cells were washed and then counted without lysis.

### Cell Identification and Flow Cytometry

To identify and sort the specific cell populations by flow cytometry, a series of monoclonal antibodies (BD Biosciences), including anti-CD19 PE-Cy7, anti-TCR APC, anti-CD4 FITC, anti-CD8 PerCP, anti-CD11b FITC, and anti-Ki67 PE, were used to mark cells. Samples from splenic cells and lymph node cells were subjected to surface staining by incubating them with a specific antibody on ice for 30 min in the dark<sup>[26-27]</sup>. Cell identification and sorting were conducted with a FACS Canto II and FACS Aria Cell Sorter. Data were analyzed with Flow Jo software. T lymphocytes, B lymphocytes, and myeloid cells were separated by incubating them with anti-TCR APC, anti-CD19 PE-Cy7, and anti-CD11b FITC. T lymphocytes were identified as CD4+ and CD8+ cells by incubation with anti-CD4 FITC and anti-CD8 PerCP antibodies. CD19+ cells, CD4+ cells, and CD8+ cells were then incubated with anti-Ki67 PE to assess cell activation.

### Splenic Lymphocyte Proliferation and Apoptosis

To evaluate lymphocyte proliferation, about  $2 \times 10^5$  cells from one sample were added to 100  $\mu\text{L}$  RPMI-1640 complete culture medium [containing 10% fetal bovine serum (Corning) and 1% penicillin-streptomycin (Solarbio)]. Then, phorbol-12-myristate-13-acetate (PMA, Sigma) and ionomycin (Iono, Abcam) were added in 100  $\mu\text{L}$  1,640 complete culture medium to achieve a concentration of 200 ng/mL and 2,000 ng/mL. After mixing the two solutions in each well, the plate was incubated at 37 °C in a humidified atmosphere with 5%  $\text{CO}_2$  for 3

days. A Cell Counting Kit (CCK8 kit, Dojindo) was used to quantify cell proliferation. After carefully removing the upper cell culture medium, 10  $\mu$ L CCK8 and 90  $\mu$ L 1,640 complete culture medium were added to each well. After 1 h of incubation, the cells in each well were mixed, and the absorbance was measured at 450 nm with a microplate reader.

To quantitatively measure the activation-induced cell death of splenic lymphocytes, an Annexin-V-FLUOS Staining Kit (Roche) was employed<sup>[28]</sup>. The following steps were conducted according to the manufacturer's specifications. Annexin-V-FLUOS label solution, which contains annexin-V-FLUOS, propidium iodide (PI), and HEPES buffer, was prepared. After incubation with PMA and Iono as in the proliferation assay, cells were washed twice with PBS and incubated with the annexin-V-FLUOS label solution in the dark at room temperature (RT). About 30 min later, cell suspensions were detected with FACS Canto II.

### ELISA

The sera samples were analyzed with a double antibody sandwich ELISA to measure IgM and IgG concentrations. Microtiter 96-well plates were coated with 0.5  $\mu$ g/mL goat anti-mouse IgG (Millipore)/rat anti-mouse IgM (BD Biosciences) and incubated at 4 °C overnight. The next day, the plates were washed with PBST (PBS containing 0.05% tween-20) three times<sup>[29]</sup>. Non-specific binding sites were blocked by 1% (w/v) bovine serum albumin (BSA) in PBS at RT for 2 h. Diluted test sera ( $10^5$  dilutions for IgG test and  $10^4$  dilutions for IgM test) and double-diluted (maximum concentration was 100 ng/mL) IgG (Invitrogen)/IgM (BD Biosciences) isotype control were added to these wells, followed by incubation at RT for 2 h. After washing six times with PBST, 1000-times diluted goat anti-mouse peroxidase conjugated IgG/IgM (Sigma) was added to each well and left at RT for another 2 h. The plates were washed six times again, and 3,3',5,5'-tetramethylbenzidine (TMB) was added for oxidation by peroxidase. The reaction was stopped by 2 mol/L sulfuric acid ( $H_2SO_4$ ) solution after 10 min (for IgG) or 20 min (for IgM)<sup>[29-30]</sup>. Absorbance values were read at 450 nm with a plate reader. Of note, the plates were dried enough before adding another solution.

### Histology

After fixation, the skin samples were dehydrated, embedded in paraffin, and sectioned according to

standard procedures. Thereafter, paraffin blocks were cut into 3-5  $\mu$ m sections and mounted on glass slides and then deparaffinized and stained with hematoxylin and eosin (H&E) according to routine processing procedures to assess total cell infiltration<sup>[23-24,31]</sup>.

### Immunohistochemistry

Immunostaining of IFN- $\gamma$  and TNF- $\alpha$  was used to identify the tissue inflammatory response. For immunostaining, 3-5  $\mu$ m paraffin-embedded sections were mounted on glass slides. As previously reported<sup>[32-33]</sup>, the slides were deparaffinized, hydrated, and permeabilized with 3% hydrogen peroxide to quench endogenous tissue peroxidases. Subsequently, the slides were rinsed and blocked with 5% BSA and incubated with the primary antibody overnight at 4 °C. For staining, the slides were incubated with a biotin-conjugated secondary antibody. Post-washing, the slides were then incubated with avidin and biotinylated horseradish peroxidase. After they were rinsed, a color reaction was induced on the slides by adding 3, 3'-diaminobenzidine (DAB), after which they were counterstained with hematoxylin. Subsequently, the slides were dehydrated, made transparent, and mounted. The stained slides were examined, and images were captured with an optical microscope.

### Statistical Analysis

All data analyses were conducted in GraphPad Prism version 6, and data are expressed as the mean  $\pm$  standard error of mean (SEM) from at least three mice. Data following a Gaussian distribution were analyzed by one-way ANOVA and Dunnett's test for multiple comparisons between the NC group and the other groups. A non-parametric test, the Kruskal-Wallis test, was used to analyze data following a non-Gaussian distribution. \* $P < 0.05$ , \*\* $P < 0.01$ , and \*\*\* $P < 0.005$  were considered significant differences compared to the NC group.

## RESULTS

### Immune Organs and Cell Population

According to ISO10993-20: 2005, the weight of immune organs is a nonfunctional index of the immune response. In this study, for convenience, the size of organs, including the spleen and lymph nodes, was recorded to evaluate the intensity of the

immune response to the implants. Macroscopically, the spleens and lymph nodes of the DM groups were compared with those of the NC group and PC group. As seen in Figure 1A, the size of the spleens of the DM groups did not dramatically increase but remained a similar size as those of the NC group, which were much smaller than those of the PC group on days 7 and 60 post-surgeries. No apparent spleen size difference between the DM groups and NC group was observed at other time points (Supplementary Figure S1A available in [www.besjournal.com](http://www.besjournal.com)). In the images of lymph nodes (Figure 1B), only the lymph nodes in the PC group were noticeably swollen on day 7 or day 60, and the differences between the DM groups and NC group were minimal. A similar phenomenon was observed at the other time points (Supplementary Figure S1B). As determined by microscopy, the lymphocyte population can reflect the intensity of the immune response to a certain extent. In Figure 1C, the splenic lymphocyte populations of the DM groups were always below  $2 \times 10^8$ , maintaining minor differences with the NC group. More cells in prophase were observed in the DM-H group after three immunizations; however, the cell population steadily decreased to a normal level by day 30. The lymph node

cell counting results are shown in Figure 1D. The PC group had a considerably larger cell population than the other groups, especially on day 60, when it increased to a peak value of  $3.3 \times 10^7$ , which was almost 2-fold or more higher than those of the other groups. Notably, the number of lymphocytes in the DM-H group on days 7 and 14, ranging from  $1.7 \times 10^7$  to  $2 \times 10^7$ , approached the level of the PC group, but it did not increase sequentially and decreased to the level of the NC group. In contrast to the DM-H group, the DM-L group had no visible difference from the NC group over the 90 day post-implantation period. These results illustrate that DM-H evoked mild cell proliferation in the early period post-implantation, which was more obvious than the response evoked by DM-L, indicating that DM-H likely triggered a moderate but temporary immune response.

Cell Phenotype

In ISO 10993-20: 2005, cell phenotype is an important nonfunctional method to identify cell subsets that mediate inflammation and cellular and humoral immune responses. To assess the immunogenicity of DM, the impact of DM subcutaneous implantation on the splenic and lymph

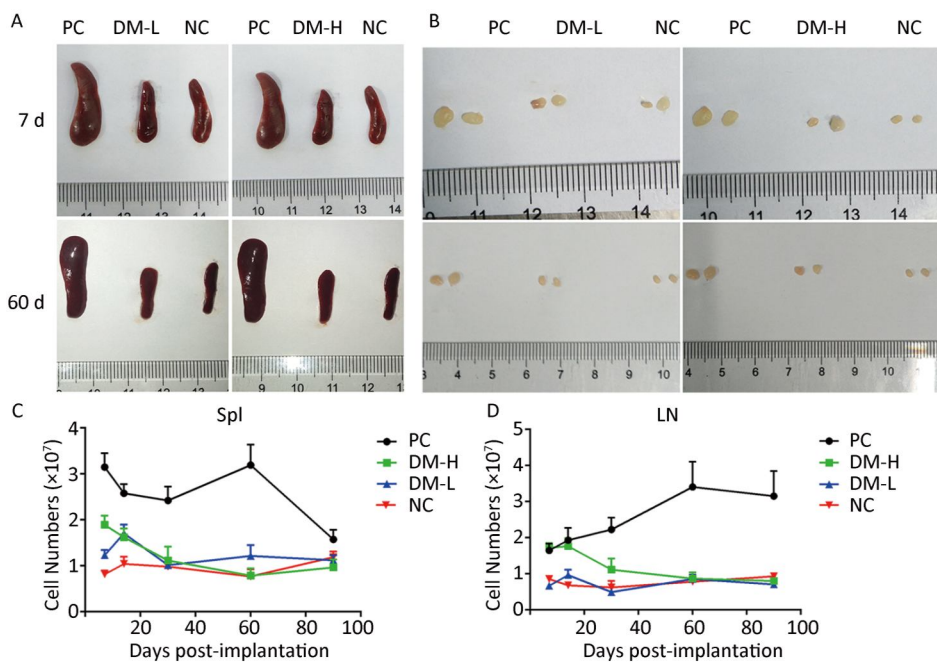


**Figure 1.** Images of the spleen (A) and lymph nodes (B) on days 7 and 60, as well as their cell populations (C, D) at different harvesting time points. In each image, the spleens and lymph nodes are placed in the order of PC, DM, and NC from left to right. Data are expressed as the mean ± SEM, *n* ≥ 3. Spl: spleen; LN: lymph nodes.

node cell subpopulations was investigated. Cell subsets, including T, B lymphocytes (mediating cellular and humoral immune responses, respectively), and CD11b+ cells (because they are an indication of an innate immune response), in the spleens from the DM groups exhibited small changes over time (Figure 2). Briefly, on day 7 (Figure 2A), the TCR+ lymphocyte number in the DM-H group, which was similar to that in the PC group, was about twice that in the NC group, a difference that was significant ( $P < 0.05$ ); the DM-H group also had a significantly ( $P < 0.01$ ) higher CD19+ lymphocyte population than the NC group. However, the DM-L group was not significantly different from the NC group, and the CD11b+ myeloid cell populations also did not noticeably change following DM implantation. Up to day 60 (Figure 2B), the DM groups maintained small differences with the NC group for the three cell subsets, although the TCR+ cell population in the DM-H group remained significantly higher than that in the NC group ( $P < 0.01$ ). Compared to the difference between NC group and PC group, the differences between the DM groups and NC group obviously decreased, for all cell subsets. T and B lymphocytes in the lymph nodes from mice in the DM groups did not exhibit significant abnormalities on day 7, but a slightly higher cell population was observed in the DM-H group compared to that in the PC group (Figure 3A). However, this difference became minimal on day 60 (Figure 3B), unlike in the PC group, which had 2-fold

and 4-fold higher T and B cell populations than the NC group. These findings indicate that cell subsets related to the adaptive immune response in the spleen and lymph nodes were initiated weak and transient composition abnormalities following the implantations of DM, and the effects of DM-H were more apparent.

**Splenic Cell Ki67 Expression**

Ki67 is an antigen associated with cell proliferation. To investigate splenic cell activation stimulated by DM implantation, Ki67 expression in lymphocytes was analyzed by immunofluorescent staining and flow cytometry. In the current study, Ki67+ splenic CD4+, CD8+, and CD19+ lymphocytes were found at all times in all groups (Supplementary Figure S2 available in [www.besjournal.com](http://www.besjournal.com)). As shown in Figure 4, the Ki67 expression rates of CD4+, CD8+, and CD19+ cells in mice with DM implants were close to those in normal mice without implants on day 60; however, the rate in the DM-H group was marginally higher than that in the DM-L group, and those in PC mice were much higher than those in the NC group. In overall, in mice implanted with DM or nothing, CD4+ and CD8+ lymphocytes in the spleen maintained relatively constant proliferation proportions from days 7 to 90, while in mice implanted with bovine tendon, the proliferating CD4+ and CD8+ lymphocyte proportions keep increasing over the 60 days post-implantation and

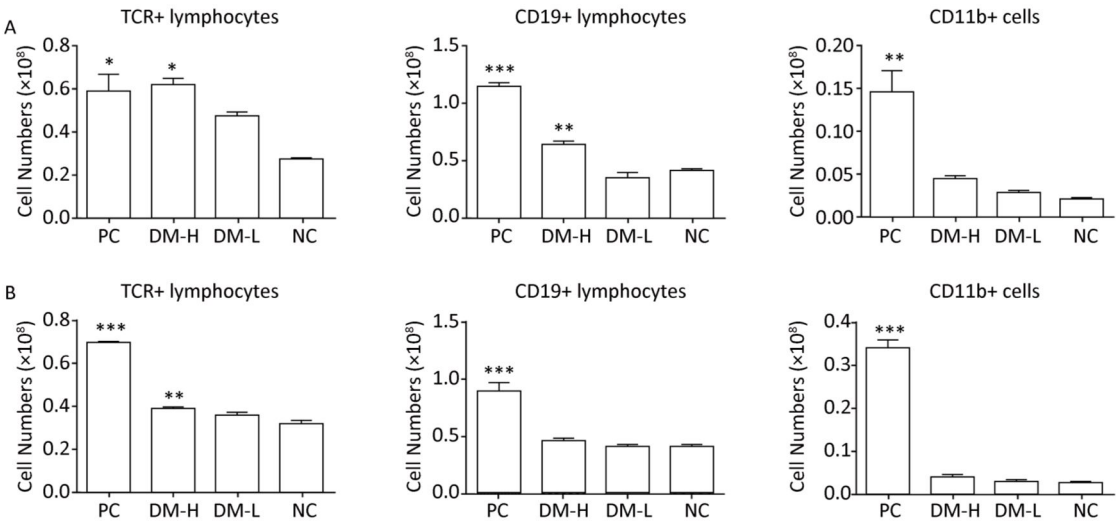


**Figure 2.** Splenic TCR+, CD19+, and CD11b+ cell subpopulations on days 7 (A) and 60 (B) following three immunizations. Data were calculated from the results of cell counting and flow cytometry plots. Data are expressed as the mean  $\pm$  SEM,  $n \geq 3$ . \* $P < 0.05$ , \*\* $P < 0.01$ , and \*\*\* $P < 0.005$ , indicate significant differences from the NC group.

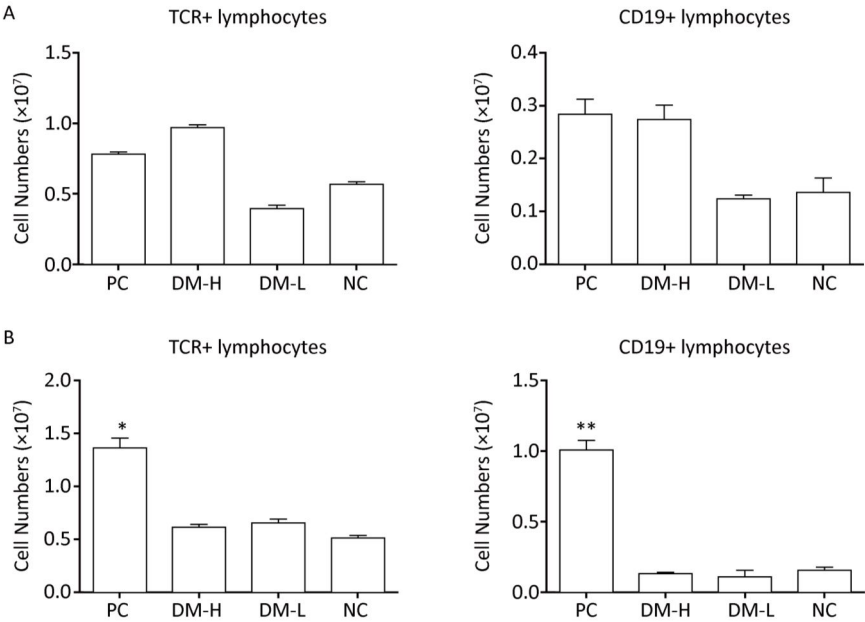


**Figure 3.** TCR+ and CD19+ cell subpopulations in lymph nodes on days 7 (A) and 60 (B) following three immunizations. Data were calculated from the results of cell counting and flow cytometry plots. Data are expressed as the mean ± SEM, *n* ≥ 3. \**P* < 0.05 and \*\**P* < 0.01 indicate significant differences from the NC group.

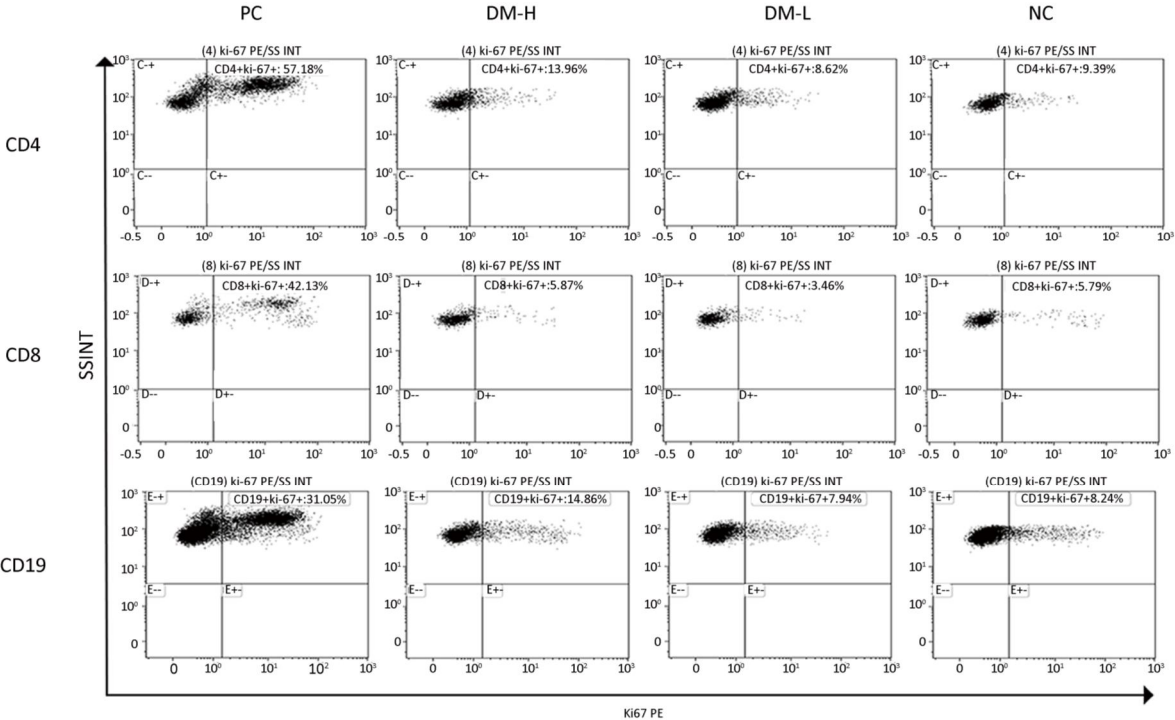


**Figure 4.** Splenic cell activation determined by Ki67 expression. Ki67 antigen expression was detected by cell immunofluorescence staining with anti-Ki67 PE. Representative flow cytometry plots of Ki67 staining showing the Ki67+ cell percentage in CD8+, CD4+, and CD19+ lymphocytes on day 60 post-implantation.



reached peak values at day 60 (Supplementary Figure S2). For the proportion of CD19+ cell activation, a higher proportion was found in all groups on day 14 than at other times (data for day 7 were not obtained), but the difference was not remarkable (Supplementary Figure S2). Collectively, there was no significant difference ( $P < 0.05$ ) between the DM groups and NC group at any sampling time point, indicating that the immune response triggered by DM in mice was extremely mild.

**Splenic lymphocyte Proliferation and Apoptosis *ex vivo***

As indicated in ISO 10993-20: 2005, the immune response can be evaluated by cell proliferation, which is a functional assay for T and B lymphocytes. For determining the activation extent of splenic lymphocytes after the immunizations with DM, PMA and Iono were used to stimulate lymphocyte proliferation *ex vivo*. Figure 5A-D summarize the results of lymphocyte proliferation. On day 7, cell proliferation in the PC and DM-H groups was significantly higher than that in the NC group, as the absorbance was 7-fold and 3-fold higher, respectively (Figure 5A,  $P < 0.005$ ). By day 14, this difference in absorbance between the DM-H group

and NC group markedly decreased (Figure 5B). In the late post-implantation period, there remained no differences in proliferation between the DM groups and NC group, as all had an absorbance value of 0.2 (Figure 5C, D, data for day 30 were not successfully obtained). In contrast, during the entire experimental period, cell proliferative ability of the PC group was greatly higher than that of the NC group. In general, the cell proliferative ability of the DM groups decreased, as indicated by the loss of the difference from the NC group; thus, we conclude that a mild acute immune response may have occurred after DM implantation. Regarding the dose effect, splenocytes in mice stimulated with DM-H were more capable of proliferating *in vitro* than those in mice stimulated with DM-L on days 7 and 14, demonstrating that the BALB/c mice were slightly more responsive to DM-H than to DM-L.

In order to analyze cell activation triggered by DM implantation, another functional index, the activation-induced cell death level, was tested after stimulation with PMA and Iono *ex vivo*. As shown in Figure 5E, the cell apoptosis percentages in all groups, even the PC group, were similar on day 7 post-immunization, as the differences were not statistically significant ( $P > 0.05$ ). Similar apoptosis outcomes were obtained at the other harvesting time

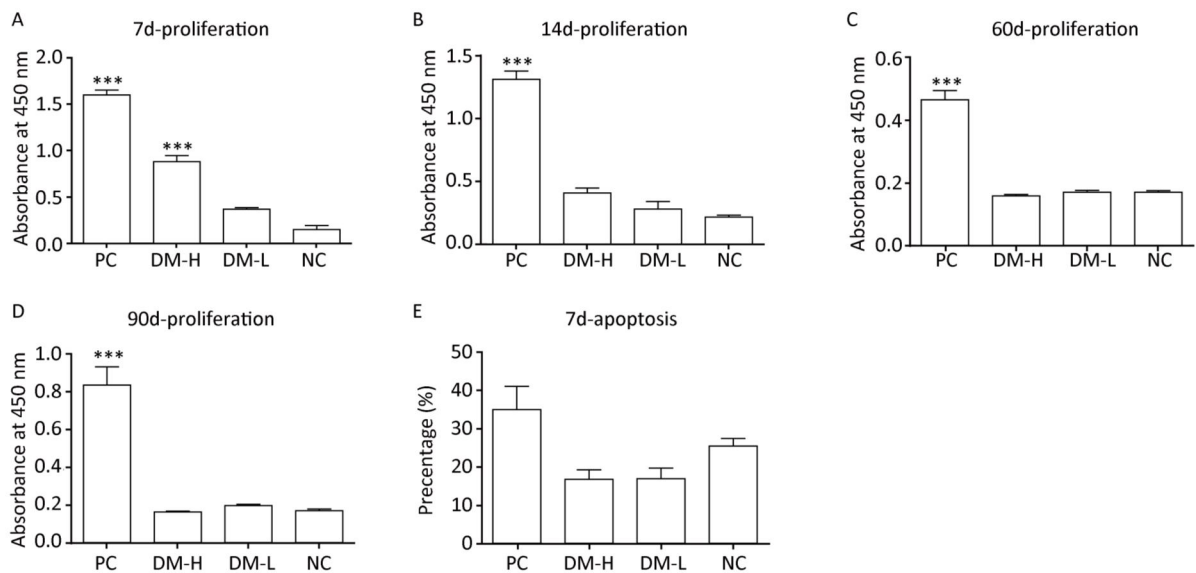


**Figure 5.** Splenic lymphocyte activation level after three immunizations by assessing cell proliferative ability and apoptosis level *in vitro*. Splenic lymphocyte proliferation *in vitro* on days 7 (A), 14 (B), 60 (C), and 90 (D) post-implantation and apoptosis *in vitro* on day 7 (e) post-implantation were determined following stimulation with PMA and Iono for 3 days and quantification with a CCK8 kit and Annexin-V kit. Data are shown as the mean  $\pm$  SEM of at least three samples. \*\*\*  $P < 0.005$  indicates a significant difference from the NC group.



points. Although this phenomenon was not expected, we suspect it may be explained by the extensive death of NC lymphocytes by excessive unspecific stimulation.

**Total Serum IgG and IgM Level**

ELISA is a very common method for testing the humoral immune response in ISO 10993-20: 2005. To verify the humoral immune response intensity induced by different doses of DM, the immunoglobulin concentration in the sera of immunized mice at different times was determined by ELISA, as elevated immunoglobulin concentration is a sign of B cell activation. IgM is the first secreted antibody in the immune response; hence, it was only detected on days 3, 7, and 14, whereas IgG is produced later than IgM. IgM concentration changes after the implantations are shown in Figure 6A. Bovine tendon clearly elicited an aggressive response as indicated by the large amount of IgM secreted, reaching 1,000  $\mu\text{g/mL}$  after 3 days. Compared with response to bovine tendon, IgM secretion triggered by DM was modest, remaining at 250  $\mu\text{g/mL}$  or lower, comparable to that in normal mice. Moreover, there was no apparent IgM concentration difference between the DM-H group and DM-L group. Similarly, as shown in Figure 6B, there was no obvious IgG concentration difference between the DM groups and NC group, all fluctuating around 5  $\text{mg/mL}$ , but a marked difference was observed between the PC group, with a peak value of 30  $\text{mg/mL}$  on day 30 following the immunizations, and the other groups (Figure 6B). These outcomes indicate that the DM material induced less antibody secretion than bovine tendon

and resulted in an antibody concentration comparable to that in the group with no implant, indicating that DM evoked a minimal humoral immune response.

**Local Immune Response**

The above examinations reflect the systemic immune response, so the following tests focused on the local cellular response. Hypersensitivity is excessive immune response to a repeated stimulation with an antigen after being sensitized by the antigen. Delayed type hypersensitivity (DTH), mediated by T lymphocytes and monocytes, can be evoked by implants after 24 h, and it was evaluated in this study using cell infiltration and cytokine expression at local implantation sites. Cell infiltration is an effective method to evaluate local reactions in ISO 10993-6.

**Cell Infiltration Around Implants** To evaluate the immunogenicity of DM, total cell infiltration, mainly infiltration of T lymphocytes and macrophages, was examined by H&E staining. Figure 7 presents representative H&E staining images of the implantation sites. As shown, the obvious infiltration of cells was found around DM on day 7 following implantations (Figure 7B, C) and around bovine tendon on days 7 and 60 (Figure 7A, E). However, on day 60, almost no inflammatory cells infiltrated around DM (Figure 7F, G). In fact, DM clearly attracted cell infiltration into the area surrounding it in 30 days post-implantation (Supplementary Figure S3 available in [www.besjournal.com](http://www.besjournal.com)). The differences between PC and DM included not only a much smaller cell infiltration area, but also the temporality of cell infiltration in the DM slides, especially

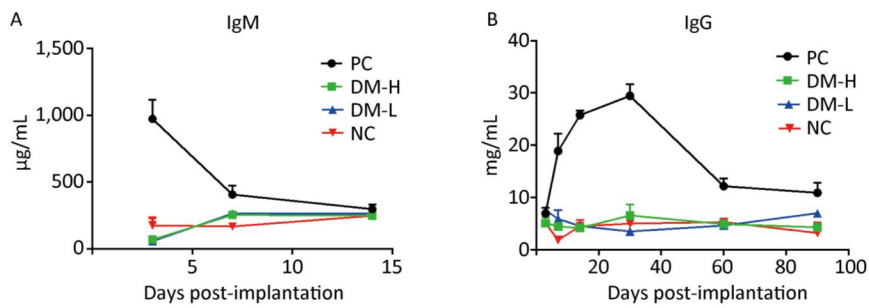


**Figure 6.** Humoral immune response of mice to implants following three immunizations. Double antibody sandwich ELISA was used for IgM (A) and IgG (B) concentration quantification in the peripheral blood of mice. Data are expressed as the mean  $\pm$  SEM from at least three sera samples per group per time point.

in the DM-L slides. This outcome is accordant with the former conclusion, that DM implantation initiated a benign transient immune response.

**IFN- $\gamma$  Expression** To investigate the DTH immune response level at local sites, IFN- $\gamma$ , which is primarily secreted by activated T lymphocytes and NK cells to promote inflammation, was assessed by immunostaining. Weak IFN- $\gamma$  immunostaining was observed in all groups (Supplementary Figure S4 available in [www.besjournal.com](http://www.besjournal.com)). IFN- $\gamma$  staining in the DM-L group and DM-H group was comparable to that in the NC group on day 7 and day 60 (Figure 8). Moreover, no difference in immunostaining intensity between the NC group and the two DM groups was noticeable at any time point (Supplementary Figure S4). These findings indicate

that the DTH engendered by DM subcutaneous implantation was so weak that it could not be detected with this index.

**TNF- $\alpha$  Expression** The expression of TNF- $\alpha$ , a proinflammatory cytokine, was also evaluated to analyze the DTH level. As shown in Figure 9, there were markedly smaller areas of positive staining (blue arrows) in slides from the DM-L and DM-H groups on day 7 compared to those in slides from the PC group, in which there is widespread staining around implants. Moreover, TNF- $\alpha$  expression in the DM-L and DM-H groups decreased over time (Supplementary Figure S5 available in [www.besjournal.com](http://www.besjournal.com)). By day 60, the difference between the DM groups and NC group had disappeared (Figure 9F, G, H). However, TNF- $\alpha$  expression in the PC group did

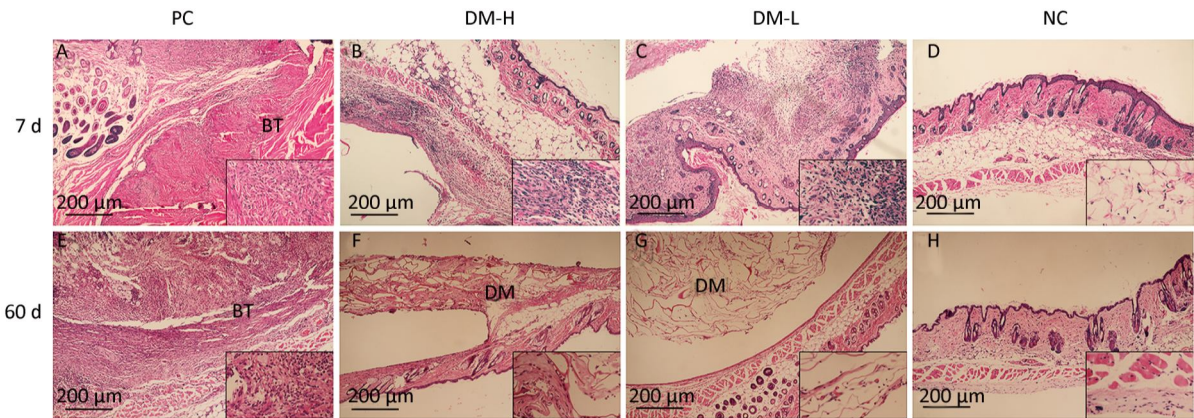


**Figure 7.** Cell infiltration around implants. Skin samples from implantation sites were cut out, and cell infiltration was determined by H&E staining. Representative images of cell infiltration around implants on days 7 (A-D) and 60 (E-H) after three immunizations, indicating inflammation intensity and duration. Nuclei are stained blue, and the cytoplasm, connective tissues, and muscles are stained red by H&E staining. All sections were examined with an optical microscope. BT: bovine tendon, DM: dermal matrix.

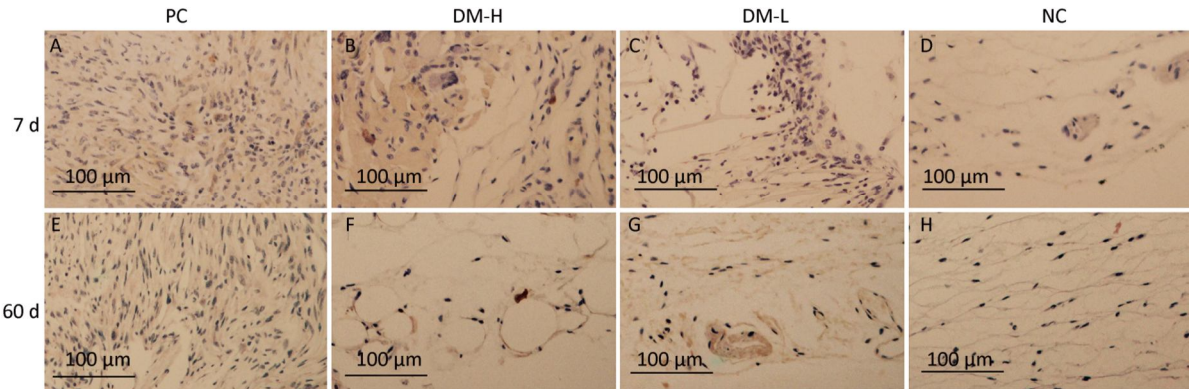


**Figure 8.** Effects of DM implantation on proinflammatory cytokine (IFN- $\gamma$ ) expression. IFN- $\gamma$  expression at implantation sites was determined by immunohistochemistry. Representative images of IFN- $\gamma$  immunostaining around implants on days 7 (A-D) and 60 (E-H) post-surgeries are displayed. All sections were imaged with an optical microscope.

not obviously subside from day 7 to day 90. These results also indicate that the immune response engendered by DM implants was marginal and transient.

DISCUSSION

It should be noted that the immune response elicited by implants might cause severe clinical symptoms. Although collagen is believed to have low immunogenicity, adverse reactions, such as local hypersensitivity, do occur in the clinic after the use of collagen products<sup>[14]</sup>. Therefore, it is necessary to investigate the immunological reaction induced by any new collagen product. Here, we studied a type of bovine collagen dermal regeneration matrix. We aimed to thoroughly and comprehensively study the immune response aroused by the material, predicting that it would produce only slight or no host responses to lay the foundation for future clinical trials.

As previously described, multiple collection time points are recommended for anti-drug antibody assessments, and the number of time points should be selected to provide statistically meaningful data for the immunogenicity assessment. Additionally, the highest dose and the most sensitive population are also recommended to achieve the strongest immune response<sup>[34]</sup>. Similarly, these factors were considered in our scheme to evaluate the immunogenicity of the collagen-based dermal substitute. The low dose was calculated based on the maximum single dose and body surface area ratio of BALB/c mice and humans, and it was

one-fourth of the high dose. The longest sampling time (90 days) was the degradation time of DM according to our previous study. Moreover, the experimental animals were 6- to 8-week-old BALB/c female mice. Because BALB/c mice are sensitive to antigens, the females can produce more antibodies than the male, and the younger mice have a greater immune responsive ability than the older and infant mice. We aimed to induce the strongest possible immune response in BALB/c mice with DM-H implants. A benign immune response would be an indication of the extremely low immunogenicity of the DM. Furthermore, this study focused on adaptive immunity, as the innate immune response occurs early after implantation; our study included three implantations, therefore the adaptive immune response was the predominant reaction and was investigated comprehensively. However, the innate immune system can regulate adoptive immunity<sup>[35]</sup>; thus, innate immunity was also approximated.

According to ISO 10993-20: 2005, predicting the immunotoxicity of new chemicals and materials is difficult, therefore effort and interest need to be focused on the assessment and management of risks. Risk assessment includes hazard identification, dose response assessment, and exposure assessment. Immunological hazards should be identified by assessing exposure to medical device materials to identify the presence of (potentially) immunotoxic agents, and related *ex vivo* tests were evaluated prior to this study. Dose response assessment and exposure assessments were performed in this study. ISO 10993-20: 2005 also indicates that a medical

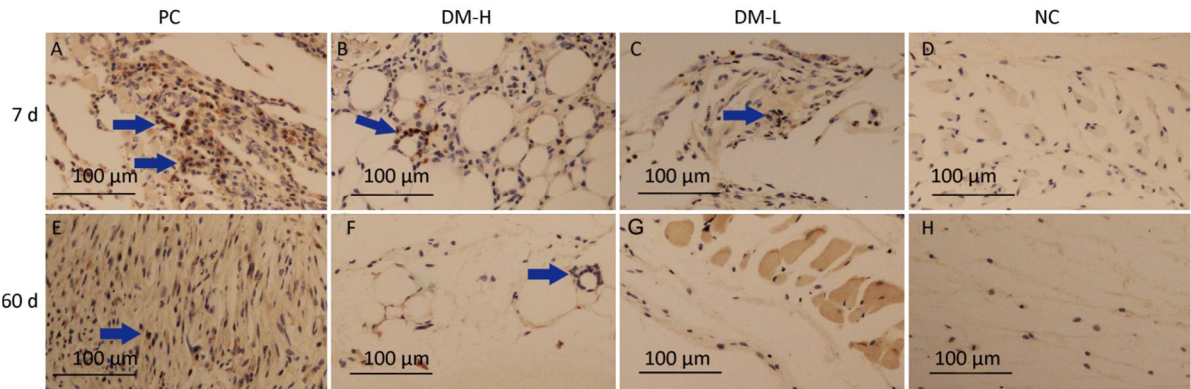


**Figure 9.** Effects of DM implantation on proinflammatory cytokine (TNF-α) expression. TNF-α expression at implantation sites was determined by immunohistochemistry. Representative images of TNF-α immunostaining around implants on days 7 (A-D) and 60 (E-H) post-immunizations are displayed. All sections were examined with an optical microscope. Positive staining is marked with blue arrows.

device implant may induce acute or chronic inflammation, hypersensitivity, immunostimulation, immunosuppression, and autoimmunity. However, immunostimulation and immunosuppression tests should be restricted in general immunotoxic studies, except for those on materials that have been shown to possibly induce immunostimulation and immunosuppression. Bovine collagen is proven nontoxic and can be well tolerated in animal models as well as in the clinic. Therefore, we mainly evaluated the systematic immune response, local inflammation, hypersensitivity, and dose response. Evaluation indexes in this study were set according to the instructions in ISO 10993-20: 2005 and previous literature<sup>[20]</sup>, though the evaluation scheme also has some weaknesses, such as insufficient functional tests, control selection, and lack of complement detection.

When an antigen enters the body, T lymphocytes and B lymphocytes may be stimulated and start to proliferate rapidly, strongly initiating the acquired immune response. The spleen and lymph nodes are the main locations where lymphocytes settle, as well as the primary regions of the immune response. In accordance with the instructions of ISO 10993-20: 2005, lymphoid organs were chosen to assess the immune response. In this study, the spleen and lymph nodes, as systematic immune response indexes, were studied according to size, cell population, cell phenotype, and activation level to evaluate the immunotoxicology of this collagen-based DM. The cell population of the DM-H group slightly increased in the early time phase (Figure 1C, D). In addition, other two tests, lymphocyte proliferation *in vitro* following stimulation with PMA and Iono and Ki67 antigen expression in cells, can also reflect the lymphocyte activation level. The former is a functional test, and the latter is not a functional test. A difference in proliferation *in vitro* between the DM-H group and NC group was also discovered, as indicated by the proportion of splenic lymphocytes in prophase after immunizations (Figure 5). The cell phenotype of the spleen and lymph nodes indicated a weak but evident alteration on day 7 in the DM-H group. These results suggest that DM-H produced some level of immune response in prophase, however over time, the collagen triple-helical structure was destroyed, collagen degraded into small pieces, and immunogenicity declined; thus, the impact on the immune system disappeared over time. However, DM-L did not trigger a noticeable immunological

reaction even in the first days after implantation. Though CD11b staining was normal in the present study, it is possible that an innate immune response occurred during the process of the three implantations because our first sampling time was 3 weeks following the first implantation.

Immunoglobulins are important effectors mediating humoral immunity, and they are secreted by plasma cells. BALB/c mice are normally used for generating antibodies against globular proteins, and they have been shown to be responsive to collagen. In one study, bovine collagen was found to be nonimmunogenic in the most responsive SJL/J mice, as the total Ig response was minimal<sup>[13]</sup>. Fish collagen was also tested in BALB/c mice, demonstrating that IgG levels in serum were also marginal on 42 days after three immunizations<sup>[18]</sup>. In the current study, the total IgG and IgM secretion of BALB/c mice response to bovine collagen DM on 3, 7, 14, 30, 60, and 90 days post-immunization was analyzed by ELISA (Figure 6). IgM and IgG concentrations in mice implanted with DM were comparable to those in normal mice with no implant and much lower than those in mice implanted with bovine tendon, in accordance with previous studies. The similarity in the immunoglobulin concentration between the DM groups and NC group illustrates that a weak humoral immune response was evoked by DM. The fluctuations in the curves can be regarded as experimental errors and individual differences in the mice.

When the body is stimulated by a foreign antigen, chemotactic factors, produced by dendritic cells, will direct inflammatory cells, mainly including neutrophils, lymphocytes, and monocytes, to exit from the bloodstream to the sites of the antigen. Generally, neutrophils play a critical role in the early phase of inflammation, and lymphocytes and monocytes are the major inflammatory cells in the middle and late phases. Inflammatory cytokines, such as TNF- $\alpha$  and IFN- $\gamma$ , primarily produced by these inflammatory cells are also secreted to regulate inflammation and the immune response. To investigate the local DTH around the implants in the present study, H&E and immunohistochemistry staining of local sites were performed. The initiation of a low level of inflammatory cell infiltration by collagen has been reported in previous studies<sup>[36-37]</sup>. Here, H&E staining revealed noticeable cell infiltration in the DM groups in the early period (Supplementary Figure S3). Noticeable cell infiltration around DM was present in the first 30



days, and then, cell aggregation subsided with the degradation of collagen, indicating that DM aroused mild acute inflammation. Collagen degradation results in a decrease in antigens, therefore inflammatory cell infiltration decreased from a large area to small dots. Regarding cytokine immunostaining, obvious TNF- $\alpha$  positive expression areas were observed in local DM implantation sites in the early phase. TNF- $\alpha$  has been reported to promote the immune response and inflammation, and it plays a critical role in inflammation in the skin<sup>[38]</sup>. However, no obvious IFN- $\gamma$  staining area was observed from day 7 to day 90 in the DM groups (Supplementary Figure S4). IFN- $\gamma$  is secreted by Th1 cells and NK cells, and its primary function is to promote the differentiation of Th1 cells, strengthen phagocytosis of phagocytes, and attract macrophages to sites where antigens are present<sup>[20]</sup>. There was no obvious IFN- $\gamma$  staining, which may reflect the poor sensitivity of the index, whereas TNF- $\alpha$  was visible in prophase, thus we propose that collagen-based DM induces a benign immune response only in the early period, as its degradation results in a weaker immunological reaction and less TNF- $\alpha$  secretion.

In summary, in the DM-H group, the cell population of the spleen and lymph nodes increased at the early time point, but did not increase in the DM-L group. As shown in Figures 2 and 3, the increase in the whole cell population in the DM-H group was primarily caused by growing T and B lymphocytes on day 7. The Ki67 results further demonstrate that the cell population increase was caused by CD4 T lymphocyte and B lymphocyte activation. A similar conclusion could be drawn from the results of the cell proliferation assay, that is the DM-H group had significantly more cell proliferation in prophase, but the DM-L group did not. Though B lymphocytes were likely slightly activated and proliferated in the above-mentioned tests by DM-H stimulation, no clear increases in immunoglobulins were detected in this study; thus, we conclude that this discrepancy is due to the quite low immunogenicity of the collagen-based DM and some experimental errors. Local cell infiltration and TNF- $\alpha$  secretion indicate that benign inflammation was evoked by DM implantation, however it was temporary. Overall, DM, especially DM-H, may have produced a slight immune response and acute inflammation in the early phase post-implantation, which then subsided gradually with the degradation of collagen. Moreover, the dose reaction evaluation

proved that the higher dose induced a more intense immune response. Therefore, the collagen-based DM can be preliminarily regarded as a reliable and safe dermal regeneration matrix with favorable biocompatibility and low immunogenicity, however dose control should not be ignored. Nevertheless, further trials must be conducted in other models and in the clinic to validate its safety. Although the research scheme proposed in this study was based on ISO 10993, there were some shortcomings, and additional studies are needed to formulate a more scientific and meaningful scheme in the future.

## ACKNOWLEDGEMENTS

The research was performed with the assistance of Peking University Health Science Center, which provided the infrastructural facility. All authors also appreciate the worker in the animal center for taking great care of the animals.

## AUTHOR CONTRIBUTIONS

NIU Xu Feng and WANG Wei designed the study together. ZHANG Lin and WANG Wei performed all experiments. SUN Lei participated in the animal surgery. SHE Zhen Ding and TAN Rong Wei provided the samples for the study. All authors reviewed the manuscript.

## COMPETING INTERESTS

The authors declare no competing financial interests.

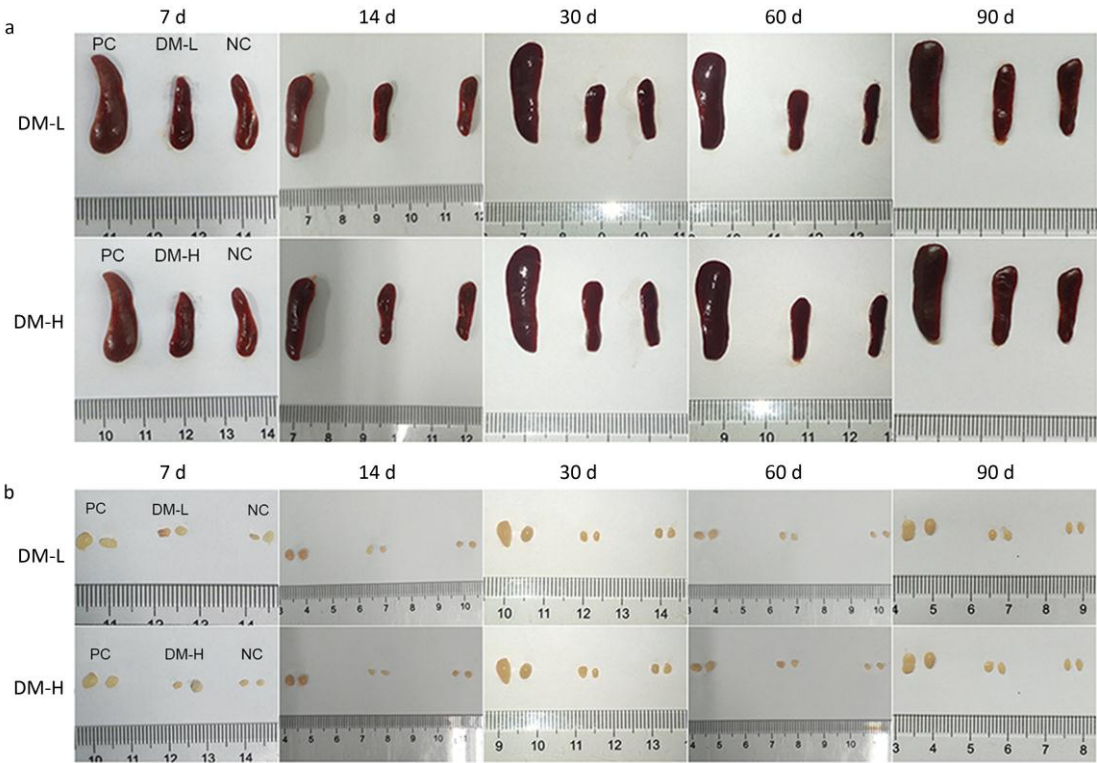
Received: February 14, 2018;

Accepted: November 22, 2018

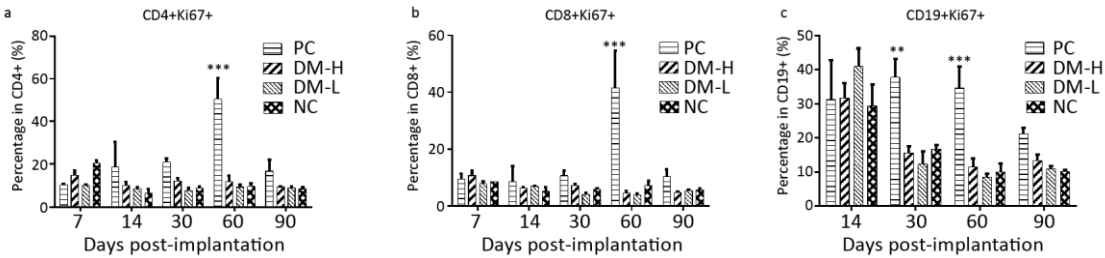
## REFERENCES

1. Colvin RB, Smith RN. Antibody-mediated organ-allograft rejection. *Nat Rev Immunol*, 2005; 5, 807-17.
2. Smolenski RT, Forni M, Maccherini M, et al. Reduction of hyperacute rejection and protection of metabolism and function in hearts of human decay accelerating factor (hdaF)-expressing pigs. *Cardiovasc Res*, 2007; 73, 143-52.
3. Puckett FA, Stahlfeld KR, DiMarco RF. Hyperacute rejection of a bovine pericardial prosthesis. *Tex Heart Inst J*, 2006; 33, 260-1.
4. Benzmira M, Calligaro GL, Glanville AR. Acute Rejection. *J Thorac Dis*, 2017; 9, 5440-57.
5. Lauro A, Oltean M, Marino IR. Chronic rejection after intestinal transplant: Where are we in order to avert it? *Dig Dis Sci*, 2018; 63, 551-62.
6. Khairuddin R, Wachtlin J, Hopfenmüller W, et al. Hla-a, hla-b and hla-dr matching reduces the rate of corneal allograft

- rejection. Graefe's Arch Clin Exp Ophthalmol, 2003; 241, 1020-8.
7. Taylor AL, Watson CJ, Bradley JA. Immunosuppressive agents in solid organ transplantation: Mechanisms of action and therapeutic efficacy. Crit Rev Oncol Hematol, 2005; 56, 23-46.
  8. Eisen HJ, Tuzcu EM, Dorent R, et al. Everolimus for the prevention of allograft rejection and vasculopathy in cardiac-transplant recipients. N Engl J Med, 2003; 349, 847-58.
  9. Souillou JP. Immune monitoring for rejection of kidney transplants. N Engl J Med, 2001; 344, 1006-7.
  10. Lee CH, Singla A, Lee Y. Biomedical applications of collagen. Int J Pharm, 2001; 221, 1-22.
  11. Gaspar A, Moldovan L, Constantin D, et al. Collagen-based scaffolds for skin tissue engineering. J Med Life, 2011; 4, 172-7.
  12. Powell HM, Supp DM, Boyce ST. Influence of electrospun collagen on wound contraction of engineered skin substitutes. Biomaterials, 2008; 29, 834-43.
  13. Peng YY, Glattauer V, Ramshaw JA, et al. Evaluation of the immunogenicity and cell compatibility of avian collagen for biomedical applications. J Biomed Mater Res, Part A, 2010; 93, 1235-44.
  14. Lynn AK, Yannas IV, Bonfield W. Antigenicity and immunogenicity of collagen. J Biomed Mater Res, Part B, 2004; 71, 343-54.
  15. Sundback CA, Shyu JY, Wang Y, et al. Biocompatibility analysis of poly(glycerol sebacate) as a nerve guide material. Biomaterials, 2005; 26, 5454.
  16. Hassanbhai AM, Lau CS, Wen F, et al. *In vivo* immune responses of cross-linked electrospun tilapia collagen membrane. Tissue Eng Part A, 2017; 23. doi:10.1089/ten.tea.2016.0504.
  17. Wang X, Tian J, Yong KT, et al. Immunotoxicity assessment of cdse/zns quantum dots in macrophages, lymphocytes and balb/c mice. J Nanobiotechnol, 2016; 14, 10.
  18. Pati F, Datta P, Adhikari B, et al. Collagen scaffolds derived from fresh water fish origin and their biocompatibility. J Biomed Mater Res, Part A, 2012; 100, 1068-79.
  19. Bornapour M, Muja N, Shum-Tim D, et al. Biocompatibility and biodegradability of mg-sr alloys: The formation of sr-substituted hydroxyapatite. Acta Biomater, 2012; 9, 5319-30.
  20. Elsbahy M, Wooley KL. Cytokines as biomarkers of nanoparticle immunotoxicity. Chemical Society Reviews, 2013; 42, 5552.
  21. Tamaddon M, Walton RS, Brand DD, et al. Characterisation of freeze-dried type ii collagen and chondroitin sulfate scaffolds. Journal of Materials Science Materials in Medicine, 2013; 24, 1153-65.
  22. Kwon HJ, Han Y. Chondroitin sulfate-based biomaterials for tissue engineering, 2016; 40, 290-9.
  23. Kim J, Dadsetan M, Ameenuddin S, et al. *In vivo* biodegradation and biocompatibility of peg/sebacic acid-based hydrogels using a cage implant system. J Biomed Mater Res, Part A, 2010; 95, 191-7.
  24. Liu H, Wise SG, Rnjak-Kovacina J, et al. Biocompatibility of silk-tropoelastin protein polymers. Biomaterials, 2014; 35, 5138-47.
  25. Fang JJ, Zhu ZY, Dong H, et al. Effect of spleen lymphocytes on the splenomegaly in hepatocellular carcinoma-bearing mice. Biomed Environ Sci, 2014; 27, 17-26.
  26. Bao LQ, Dang MN, Huy NT, et al. Splenic cd11c(+) cells derived from semi-immune mice protect naïve mice against experimental cerebral malaria. Malar J, 2015; 14, 23.
  27. O'Donnell H, Pham OH, Li LX, et al. Toll-like receptor and inflammasome signals converge to amplify the innate bactericidal capacity of t helper 1 cells. Immunity, 2014; 40, 213-24.
  28. Ge J, Liu Y, Li Q, et al. Resveratrol induces apoptosis and autophagy in t-cell acute lymphoblastic leukemia cells by inhibiting akt/mtor and activating p38-mapk. Biomed Environ Sci, 2013; 26, 902-11.
  29. Duan ZH, Lin ZA, Yao HR, et al. Preparation of artificial antigen and egg yolk-derived immunoglobulin (iyg) of citrinin for enzyme-linked immunosorbent assay. Biomed Environ Sci, 2009; 22, 237-43.
  30. Welch RJ, Litwin CM. A comparison of brucella igg and igm elisa assays with agglutination methodology. J Clin Lab Anal, 2010; 24, 160-2.
  31. Ivana M, Mhfuod EMEA, Jelena D, et al. Pulmonary immune responses to aspergillus fumigatus in rats. Biomed Environ Sci, 2014; 27, 684-94.
  32. Wang QT, Wu YJ, Huang B, et al. Etanercept attenuates collagen-induced arthritis by modulating the association between bafrr expression and the production of splenic memory b cells. Pharmacol Res, 2013; 68, 38-45.
  33. Rosenberg GA, Cunningham LA, Wallace J, et al. Immunohistochemistry of matrix metalloproteinases in reperfusion injury to rat brain: Activation of mmp-9 linked to stromelysin-1 and microglia in cell cultures. Brain Res, 2001; 893, 104-12.
  34. Liu PM, Zou L, Sadhu C, et al. Comparative immunogenicity assessment: A critical consideration for biosimilar development. Bioanalysis, 2015; 7, 373-81.
  35. Iwasaki A, Medzhitov R. Regulation of adaptive immunity by the innate immune system. Science, 2010; 327, 291-5.
  36. Shen Y, Redmond SL, Papadimitriou JM, et al. The biocompatibility of silk fibroin and acellular collagen scaffolds for tissue engineering in the ear. Biomed Mater, 2014; 9, 015015.
  37. Xiao X, Pan S, Liu X, et al. *In vivo* study of the biocompatibility of a novel compressed collagen hydrogel scaffold for artificial corneas. J Biomed Mater Res, Part A, 2014; 102, 1782-7.
  38. Wufuer M, Lee G, Hur W, et al. Skin-on-a-chip model simulating inflammation, edema and drug-based treatment. Sci Rep, 2016; 6, 37471.

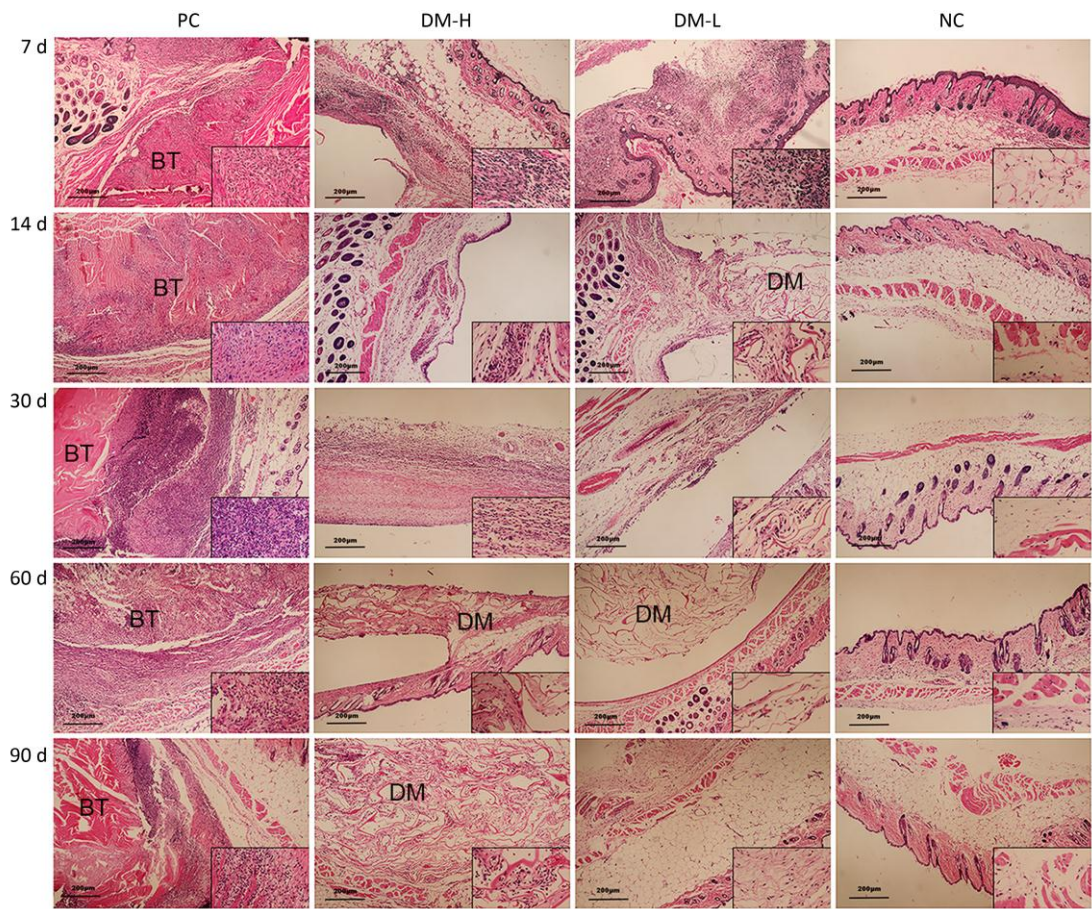


**Supplementary Figure S1.** Peripheral immune organs size at different time. Spleen (a) and lymph nodes (b) of DM groups are compared size with those of PC and NC groups. In every image, spleens and lymph nodes are put in the order of PC, DM, NC from left to right.

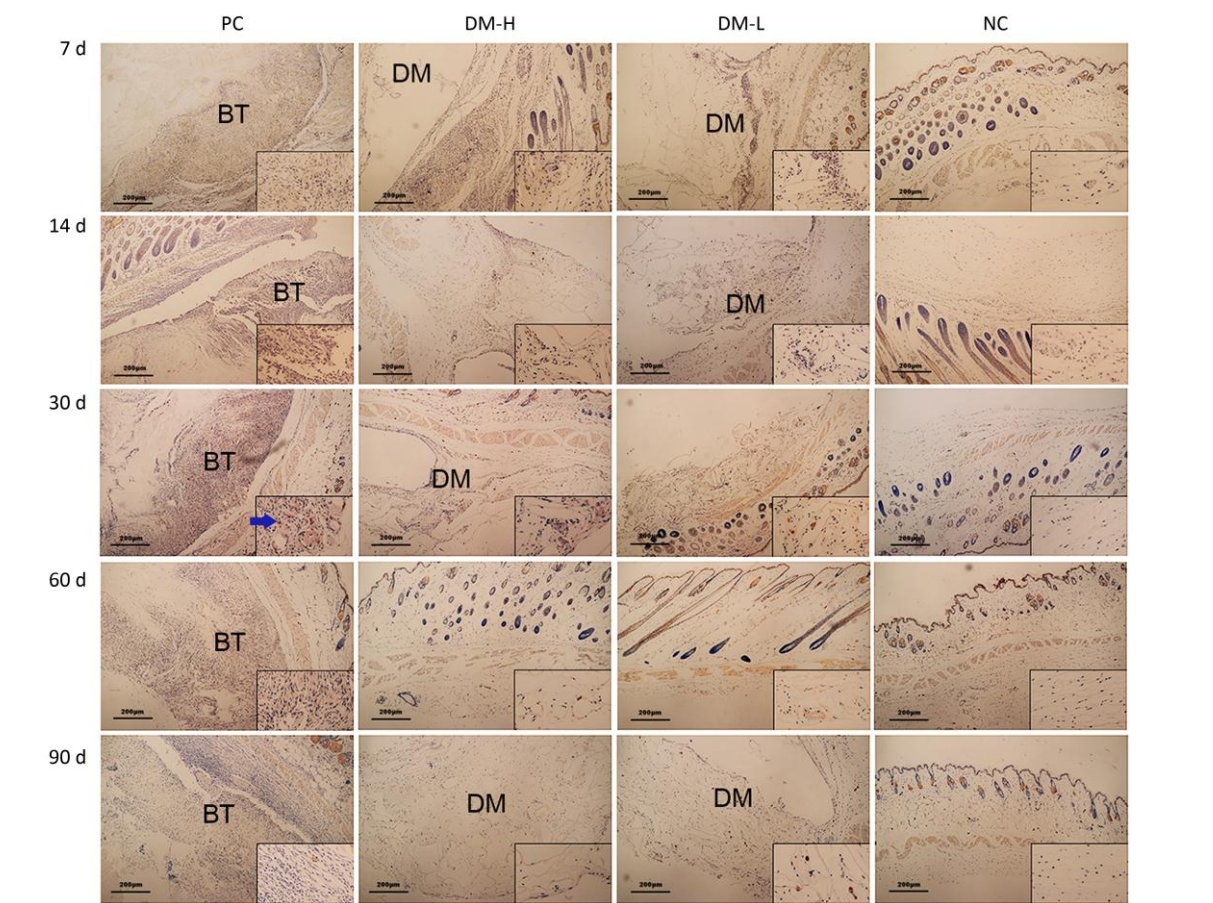


**Supplementary Figure S2.** Splenic lymphocytes activation after three immunizations was accessed by Ki67+ proportion in CD4+ (a), CD8+ (b), and CD19+ (c) lymphocytes in spleen. Splenic lymphocytes subpopulations were incubated with anti-Ki67 PE and analyzed by flow cytometry. Data are present as mean  $\pm$  SEM of at least 3 samples in every group. Difference is considered significant if \*\*  $P < 0.01$ , \*\*\*  $P < 0.005$ , compared to NC group.



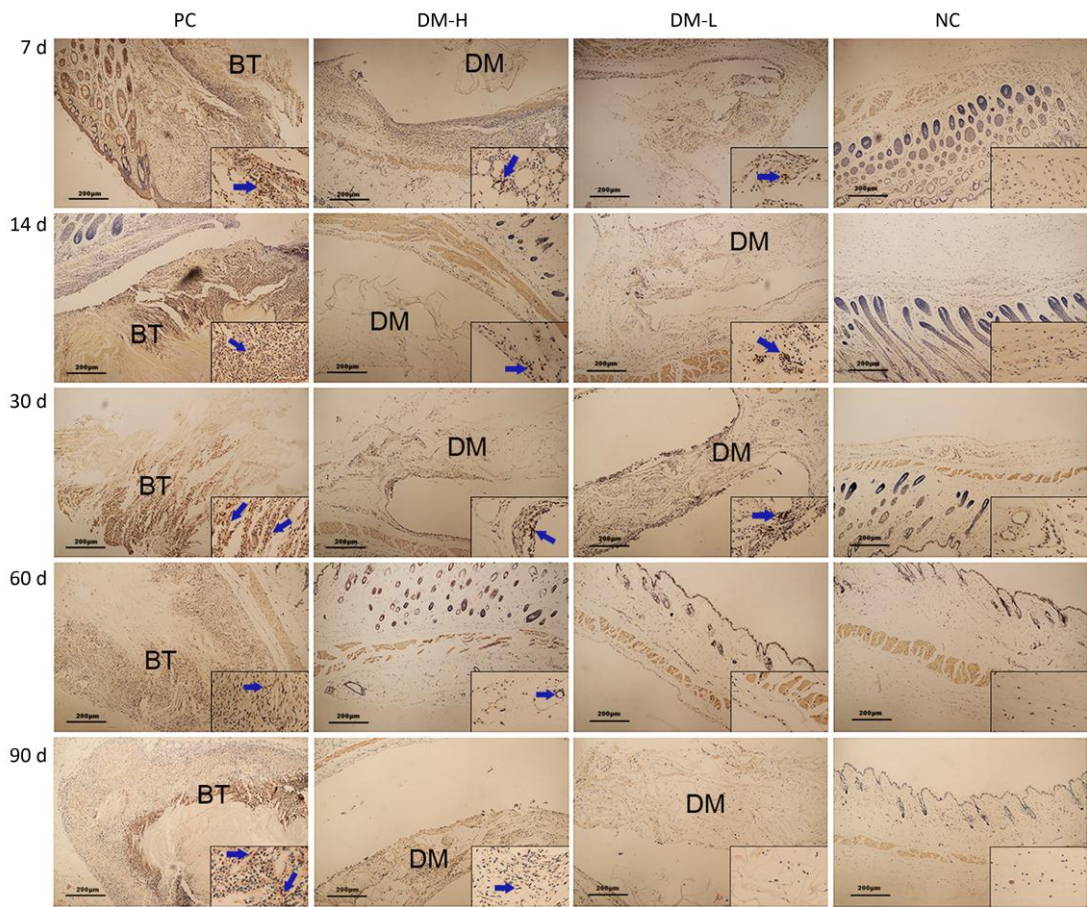


**Supplementary Figure S3.** Cell infiltration around implants. Representative H&E staining images of at least 3 samples in every group at all sampling time points are shown to analyze local inflammation reaction. Nucleus are stained blue, cytoplasm, connective tissues and muscles are stained red by H&E staining. Images were captured on an optical microscope. BT: bovine tendon, DM: dermal matrix.



**Supplementary Figure S4.** IFN- $\gamma$  expression around implants. IFN- $\gamma$  expression examination was performed by immunohistochemistry staining with anti-IFN- $\gamma$  and imaged by optical microscope. Positive staining is marked with blue arrows. BT: bovine tendon, DM: dermal matrix.





**Supplementary Figure S5.** TNF- $\alpha$  expression around implants. TNF- $\alpha$  expression examination was performed by immunohistochemistry staining with anti-TNF- $\alpha$  and imaged by optical microscope. Positive staining is marked with blue arrows. BT: bovine tendon, DM: dermal matrix.